Received: 12 September 2019 | Revised: 20 November 2019 | Accepted: 16 December 2019

DOI: 10.1111/aor.13626

MAIN TEXT ARTICLE

Artificial Organs WILEY

Circulatory loop design and components introduce artifacts impacting in vitro evaluation of ventricular assist device thrombogenicity: A call for caution

Mengtang Li[1] | **Ryan Walk**[2] | **Yana Roka-Moiia**[2] | **Jawaad Sheriff**[3] | **Danny Bluestein**[3] | **Eric J. Barth**[1] | **Marvin J. Slepian**[2,3,4]

[1]Department of Mechanical Engineering, Vanderbilt University, Nashville, TN, USA

[2]Department of Medicine, Sarver Heart Center, University of Arizona, Tucson, AZ, USA

[3]Department of Biomedical Engineering, Stony Brook University, Stony Brook, NY, USA

[4]Department of Biomedical Engineering, University of Arizona, Tucson, AZ, USA

Correspondence
Marvin J. Slepian, Department of Medicine and Biomedical Engineering, Sarver Heart Center, University of Arizona, 1501 N Campbell Ave, Tucson AZ 85724 USA.
Email: chairman.syns@gmail.com

Funding information
National Institutes of Health, Grant/Award Number: U01 1U01HL131052-01A1

Abstract

Mechanical circulatory support (MCS) devices continue to be hampered by thrombotic adverse events (AEs), a consequence of device-imparted supraphysiologic shear stresses, leading to shear-mediated platelet activation (SMPA). In advancing MCS devices from design to clinical use, in vitro circulatory loops containing the device under development and testing are utilized as a means of assessing device thrombogenicity. Physical characteristics of these test circulatory loops may also contribute to inadvertent platelet activation through imparted shear stress, adding inadvertent error in evaluating MCS device thrombogenicity. While investigators normally control for the effect of a loop, inadvertent addition of what are considered innocuous connectors may impact test results. Here, we tested the effect of common, additive components of in vitro circulatory test loops, that is, connectors and loop geometry, as to their additive contribution to shear stress via both in silico and in vitro models. A series of test circulatory loops containing a ventricular assist device (VAD) with differing constituent components, were established in silico including: loops with 0~5 Luer connectors, a loop with a T-connector creating 90° angulation, and a loop with 90° angulation. Computational fluid dynamics (CFD) simulations were performed using a $k-\omega$ shear stress transport turbulence model to platelet activation index (PAI) based on a power law model. VAD-operated loops replicating in silico designs were assembled in vitro and gel-filtered human platelets were recirculated within (1 hour) and SMPA was determined. CFD simulations demonstrated high shear being introduced at non-smooth regions such as edge-connector boundaries, tubing, and at Luer holes. Noticeable peaks' shifts of scalar shear stress (sss) distributions toward high shear-region existed with increasing loop complexity. Platelet activation also increased with increasing shear exposure time, being statistically higher when platelets were exposed to connector-employed loop designs. The extent of platelet activation in vitro could be successfully predicted by CFD simulations. Loops employing additional components (non-physiological flow pattern connectors) resulted in higher PAI. Loops with more components (5-connector loop and 90° T-connector) showed 63% and 128% higher platelet activation levels, respectively, versus those with fewer (0-connector ($P = .023$) and a 90° heat-bend

loop ($P = .0041$). Our results underscore the importance of careful consideration of all component elements, and suggest the need for standardization in designing in vitro circulatory loops for MCS device evaluation to avoid inadvertent additive SMPA during device evaluation, confounding overall results. Specifically, we caution on the use and inadvertent introduction of additional connectors, ports, and other shear-generating elements which introduce artifact, clouding primary device evaluation via introduction of additive SMPA.

KEYWORDS

computational fluid dynamics, mock circulatory loop, platelet activation, shear stress, shear-mediated platelet activation, thrombogenicity, ventricular assist device

1 | INTRODUCTION

Mechanical circulatory support (MCS) devices, that is, ventricular assist devices (VADs) and the total artificial heart (TAH) have emerged as primary therapy for patients with advanced and end-stage heart failure.[1] While effective in restoring patient hemodynamics, MCS devices remain limited by a significant persistence of device-related adverse events (AEs), with upward of 70% of patients readmitted to the hospital as a result of these AEs within 1 year of implantation.[2] A significant number of these AEs relate to altered device hemocompatibility, contributing to device-mediated thrombosis, thromboembolic events or bleeding.[2–4] A prime driver, pathophysiologically, of many of these adverse hemocompatibility-related events relates to abnormal, supraphysiologic shear stresses imparted to circulating blood within the MCS device.[5] Elevated shear stress accumulation (SA) leads to shear-mediated platelet activation (SMPA), driving thrombosis[6,7] and denaturation of von Willebrand factor, as well as other blood alterations, contributing to bleeding and disordered blood homeostasis.[8,9]

Demonstration of MCS device hemocompatibility is required for regulatory approval and subsequent human clinical use (ISO 10993-4 (2013), ISO 147808-5 (2010), and F1841-97[10]). While overall device hemocompatibility is multi-factorial,[7] a major contributor of device thrombogenicity relates to the design and geometry of flow paths within the device which lead to non-physiologic flows, turbulence, shed vortices, and the induction of SMPA.[7,11] A standard convention of device development to date has included initial in silico design optimization via computational fluid dynamics (CFD), and more recently via device thrombogenicity emulation (DTE),[12–15] followed by in vitro circulatory loop testing, prior to in vivo animal and human study.[16,17] Presently a wide variety of in vitro circulatory loop systems are in use, by both researchers and device manufacturers.[18–27] Some studies have suggested that loop geometry may affect the hemolysis and thrombosis of the MCS device under testing.[28,29] However, although some recommendations are provided by ISO 14708-5, ASTM F1841-97,[10] and FDA,[16,17] currently there is no standard design for appropriately fashioning a mock circulatory loop to minimize the rheologic impact induced by the loop itself while attempting to solely assess MCS hemocompatibility. With recent advances in the increased understanding of SMPA being dependent upon additive damage imparted to platelets,[30–32] we hypothesized that the inadvertent addition of additive connector elements and/or the alteration of loop geometry of in vitro circulatory loops may itself contribute to shear imparted to platelets leading to unanticipated additive platelet activation, with resultant inaccurate assessment of a loop-contained test MCS devices. It is understood that investigators, while careful to control for experimental system design, generally will keep all test configurations and rigs constant. However, experience in the field and practice has demonstrated frequent introduction of an additional connector here and a port there—this has been a prime motivator of this study to examine the impact of what have been deemed innocuous changes. The aim of this study was to examine, using both in silico modeling and in vitro wet studies, the impact of additive shear stress caused by complex geometry of connector components on platelet activation within MCS-testing model circulatory loops.

2 | MATERIALS AND METHODS

2.1 | In silico and in vitro VAD testing loops

A range of circulatory loops were constructed using accepted biocompatible tubing (Tygon Medical Tubing S-54-HL) and multiple types of connector components (laboratory polypropylene) varying in their geometry and application, that is, Luer connectors, angulated connectors (full details in Section 2.4 below). Schematics of these loops are shown in Figure 1. For example, a simple loop shown in Figure 1A includes two Luer connectors: one for sample collection and another for balancing the total

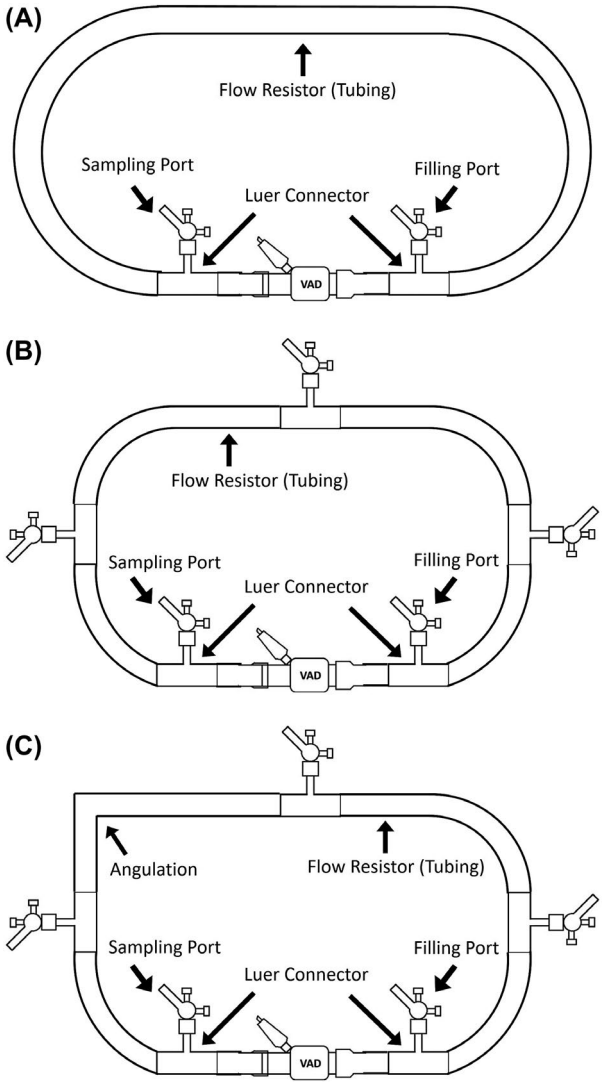

FIGURE 1 (A) A VAD testing loop with 2 Luer connectors, serving as a sampling port and a filling port; (B) a VAD testing loop with 5 Luer connectors; (C) a VAD testing loop with 5 Luer connectors and a 90° angulation

volume of the fluid circulating within the loop system. In addition to these two essential connectors, supplementary ones may also be added for other purposes such as pressure sensing (Figure 1B) or angulation (Figure 1C). Alternatively, loop angulation could be obtained by direct bending of tubing itself.

2.2 | In silico loop replication and computational fluid dynamics

In order to examine and illustrate the impact of additional shear "errors" introduced by connector geometry, eight candidate circulatory loops differing by the number of connectors or connector geometry were established in silico: loops with 0, 1, 2, 3, 4, 5 Luer connectors respectively, a loop with a T-connector to create 90° angulation, and a loop with an "ideal" 90° angulation created by tube bending. The shear stress induced by the VAD[13,14] is out of the scope of the present study and therefore is not modeled in this article. Detailed effects of the shear SA can be studied using advanced CFD/FSI simulations designed by the group.[12,13,15] All in silico testing loops were modeled to have a constant volume of 82.5 mL.

Commercial CAD software Solidworks (Dassault Systèmes, Vélizy-Villacoublay, France) was used to digitally replicate every detail of the testing loop. Figure 2A depicts a Luer connector (Qosina 27226) with a common application Tygon tube of 0.5″ ID (Saint-Gobain SA, Courbevoie, France) and Figure 2B depicts a T-connector with two sections of Tygon tubings, and their corresponding CAD models are shown in Figure 2B,E. In order to conduct the CFD calculation, the actual fluid domain geometry was digitally modeled instead of the physical solid geometry. As can be seen from the cross section view in Figure 2C,F, non-smooth regions exist at the boundary between the edge of the connector and the tubing as well as at the Luer hole. Flow patterns are more likely to be disrupted at these locations, inducing high shear regions.

Body sizing methods with high resolution were applied to the Luer connectors and angulation parts. Triangulated surface meshes and tetrahedron meshes were applied to the testing loop and a prismatic boundary with 10 inflation layers for a total thickness of 0.2 mm was added to the tubing to improve the flow resolution near the wall. A mesh density sensitivity study was conducted and a mesh with 2 million elements were found to have small deviations with finer meshes The inlet and outlet boundary conditions were set according to the in vitro experimental testing VAD HeartAssist 5 (MicroMed Technology Inc, Houston, TX, USA) which generates a flowrate of 5 LPM. The Ansys CFX CFD solver (Ansys Inc, Lebanon, NH, USA) was used to numerically solve for the $k-\omega$ shear stress transport[33,34] turbulence model based Reynolds Average Navier-Stokes (RANS) equations with a convergence criterion of RMS $< 10^{-6}$ for velocity and platelet activation transport variable.

2.3 | Scalar shear stress

Blood was treated as an incompressible non-Newtonian fluid using the Casson model with a density of 1056 kg/m^3, a yield stress of 20 mPa and an apparent viscosity of 3.5 cP.[35] The scalar shear stress (sss) σ[36] is obtained with user defined function and the correct form consistent with power law model is addressed by.[37]

$$\sigma = \left\{ \frac{1}{6} \left[(\sigma_{xx} - \sigma_{yy})^2 + (\sigma_{yy} - \sigma_{zz})^2 + (\sigma_{zz} - \sigma_{xx})^2 \right] + \left[\sigma_{xy}^2 + \sigma_{yz}^2 + \sigma_{zx}^2 \right] \right\}^{1/2} \quad (1)$$

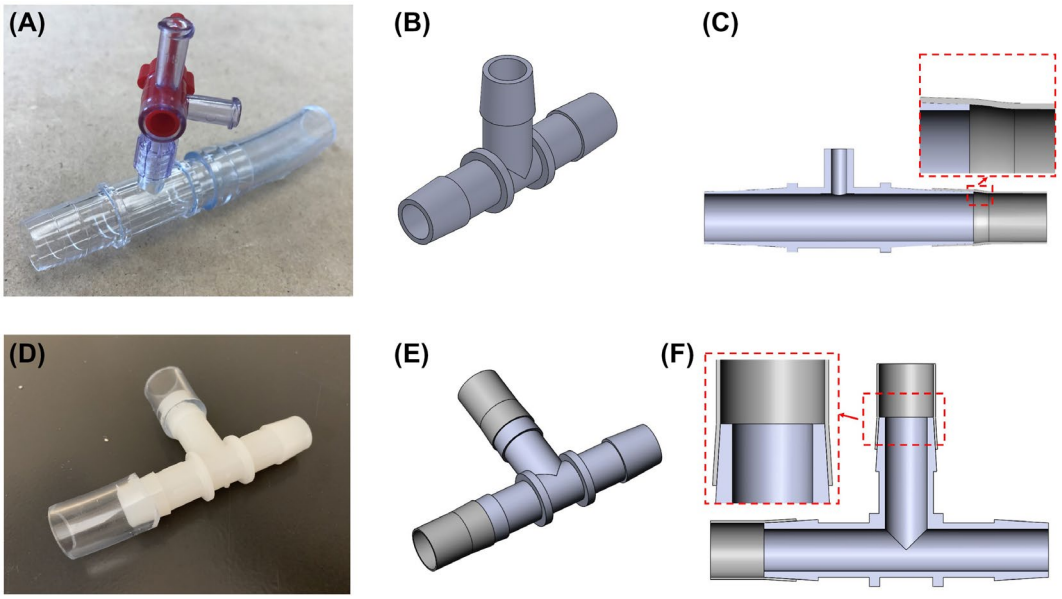

FIGURE 2 (A) A Luer connector (Qosina 27226) with a part of Tygon tubing (Saint-Gobain SA); (B) corresponding CAD model; (C) cross section view of Luer connector with a part of Tygon tubing; (D) T-connector with Tygon tubings; (E) corresponding CAD model; (F) cross section view of T-connector with Tygon tubings [Color figure can be viewed at wileyonlinelibrary.com]

Shear induced platelet activation was calculated using a well-established power law model[38]

$$PA = C\sigma^{\alpha} t^{\beta} \tag{2}$$

where coefficients C, α, β are constants obtained from experimental tests to curve fit in vitro data, σ is sss, and t is exposure time of blood. Different sets of power law constants have been obtained empirically and validated by different groups to predict platelet LDH-release, RBC Hb-release, or hemolysis etc, and here coefficients $(C, \alpha, \beta) = (4.08 \times 10^{-5}, 1.56, 0.80)$[39] were used to predict platelet activation. An Eulerian form for the PA can be obtained as

$$\frac{\partial PA'}{\partial t} + \boldsymbol{V} \cdot \nabla \mathrm{PA}' = S \tag{3}$$

where $PA' = (PA)^{1/\beta}$, $S = (C\sigma^{\alpha})^{1/\beta}$ is source term, and $\boldsymbol{V}$ is the velocity of blood. The final Platelet Activation Index (PAI) values in different scenarios were mass-weighted averaged at the outlet port.

2.4 | In vitro loop assembling

To validate previously described in silico simulations, five circulatory loops were built to be tested in vitro using a continuous flow VAD (HeartAssist V): three loops with 0, 1 or 5 Luer connectors respectively, a loop with a T-connector to create 90° angulation, and a loop with 90° angulation created by tube bending. Biocompatible medical Tygon tubing of 0.5″ ID was measured and cut according to the CAD drawing to ensure that the circulatory loops tested in vitro maximally approximate the geometry of the in silico ones and have constant volume of 82.5 mL across multiple experiments. Figure 3A depicts a loop with 5 Luer connectors with 0.5″ ID. Any one of them can serve as a filling port or sampling port. Figure 3B shows a loop with zero connectors, utilizing 2 syringe needles to fill and take samples. The effect of connector geometry on cumulative shear stress within the loop was studied through the comparison between two candidate loops. To recreate 90° angulation, either a T-connector with one end blocked (Figure 3C) was inserted or a tubing was heated utilizing a heat gun (Varitemp, Master Appliance Corp., Racine, WI, USA) until bending to the desired angle (Figure 3D). Both 90° angulation testing loops had 2 Luer connectors, at the same locations, for filling/sampling purposes.

2.5 | Isolation of human platelets

Human blood (30 mL), in accordance with University of Arizona IRB (# 1810013264) regulations, was obtained using a 21G butterfly needle (Safety-Lok, 367296) from healthy adult volunteers who were free of antiplatelet medications, including aspirin, within 2 weeks prior to blood donation, after obtaining written and informed consent prior to venipuncture. The blood was then transported in

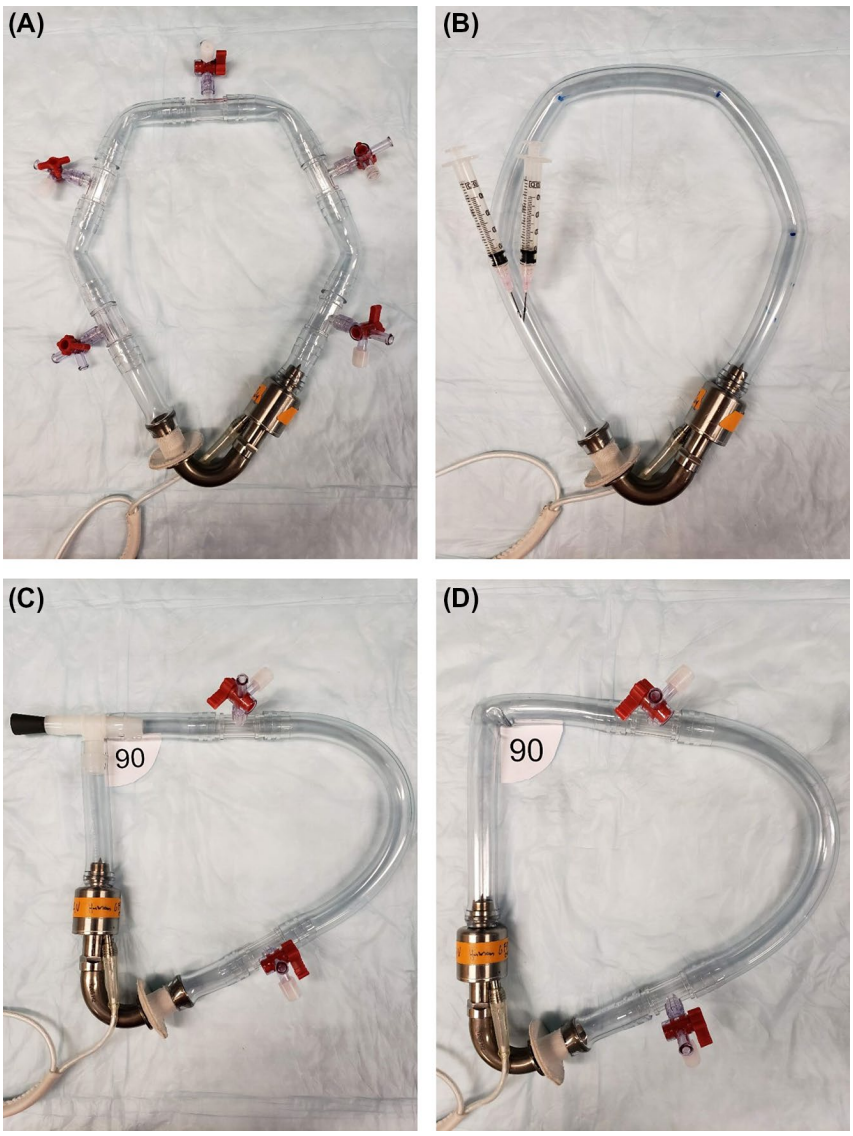

FIGURE 3 (A) in vitro testing loop with 5 Luer connectors; (B) in vitro testing loop with no Luer; (C) in vitro testing loop with 2 Luer connectors and a T-connector to create a 90° angulation; (D) in vitro testing loop with 2 Luer connectors and heat-molded a 90° angulation [Color figure can be viewed at wileyonlinelibrary.com]

polypropylene conical tube containing 3 mL of acid citrate dextrose anticoagulant solution (107 mM trisodium citrate, 60 mM citric acid, 199 mM glucose). Platelet-rich plasama was obtained by centrifugation of anticoagulated blood at 400 × *g* for 15 minutes at room temperature. Gel-filtered platelets (GFP) were isolated by filtration of platelet-rich plasma through Sepharose 2B columns equilibrated with HEPES buffer (10 mM HEPES, PH 7.4, 125 mM NaCl, 2.7 mM KCl, 2 mM $MgCl_2$, 0.5 mM NaH_2PO_4, 1 mM trisodium citrate, 25 mM glucose and 0.1% BSA). Platelet count was quantified with Z1 Coulter Particle Counter (Beckman Coulter Inc, Indianapolis, IN, USA).

2.6 | Assessing SMPA by platelet activity state (PAS) assay

Shear-mediated platelet activation was measured utilizing the Platelet Activity State (PAS) Assay, measuring thrombin generation, which has been well described and validated, both in vitro and in vivo, as a correlative and indicative marker of SMPA.[31,40,41] In brief, prior to a loop testing experiments, GFP were diluted with HEPES buffer to a final platelet count of 2×10^4/μL and recalcified (2.5 mM $CaCl_2$). Then, GFP were circulated through a tested loop at VAD operating speed around 8000 rpm for all the experiments to generate a cardiac output of 5 LPM (measured from the HeartAssist5 non-contact flowmeter), which represents the normal clinical operating range for continuous flow VADs. Platelet samples of 3 mL were collected at different times. A GFP sample incubated for 60 minutes at room temperature undisturbed was used as a negative control, while another sample activated by sonication (10 W for 10 s, Branson Sonifier 150 with microprobe, (Branson, MO, USA) served as a positive control for SMPA.[42]

The chromogenic prothrombinase-based PAS assay[40,41] was used to measure the level of platelet activation by shear

generated within the loops. A strong correlation between the level of shear stress and the level of thrombin generation by shear-activated activated platelets has been established when using acetylated prothrombin.[40] An acetylated form of thrombin cleaves a chromogenic substrate identically to native thrombin, but does not cause any feedback platelet activation. Platelet samples preliminary stimulated with shear or sonication (platelet count—$5 \times 10^3/\mu L$) were incubated with 200 nM acetylated prothrombin, 100 pM factor Xa (Enzyme Research Laboratories, South Bend, IN, USA), 5 mM $CaCl_2$ in a volume of 100 μL 20 mM HEPES, pH 7.4, containing 130 mM NaCl, and 0.1% BSA at 37°C for 10 minutes. Then, 10 μL of each timed sample was measured for thrombin activity in microplate wells, containing 0.3 mM Cromozyme TH, 3 mM EDTA in 20 mM HEPES, pH 7.4, containing 130 mM NaCl, and 0.1% BSA. Kinetic change of absorbance ($\lambda = 405$ nm) was measured for 7 minutes at room temperature using microplate reader Versa MAX (Molecular Devices Corp., Sunnyvale, CA, USA). The value of PAS or initial rate of thrombin generation was calculated as a slope of kinetic curve (ΔA405/minute) with SoftMax Pro6 Software.

2.7 | Statistical analysis

All PAS assay samples were run in duplicate. All the data were normalized to 0-min still measurement[40–42] to allow a statistically unbiased comparison and were statistically analyzed using one-way analysis of variance (ANOVA) from GraphPad Prism software (GraphPad Software Inc, San Diego, CA, USA). Averages are reported as the mean ± standard deviation. The level of statistical significance is indicated on figures as $P < .05$ (*).

3 | RESULTS

3.1 | In silico assessment of shear stresses

Straight Luer connector components were noted to impart accumulative, inadvertent shear stress, since non-smooth regions exist at the boundary between the edge of the connector and at the Luer hole. As shown in Table 1, each Luer connector created an average increase in shear stress of approximately 1.07% for one single passage of blood circulation. The distribution curves for sss of candidate circulation loops were calculated and plotted in Figure 4A. Specifically, the blood shear concentration within lower shear range (0-2 dyne/cm^2) shifts from 1 toward 1.2 dyne/cm^2 as more connectors were added to the loop. Alternatively, peak shear stress increased approximately 5.85% between non-connector and 5-connector loops, although this increase is not cumulative with each added component.

In contrast to the incremental increase of shear stress with multiple straight Luer connectors, a single T-connector to the

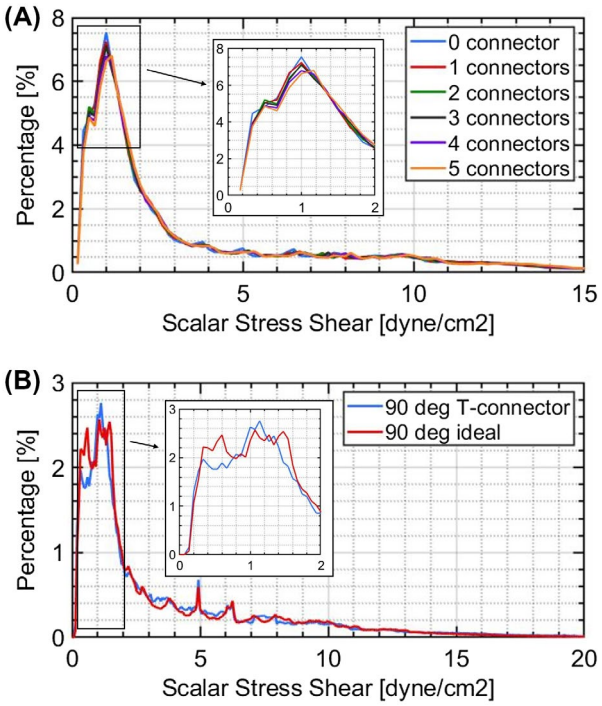

FIGURE 4 (A) scalar shear stress distribution curves for VAD testing loops with 0, 1, 2, 3, 4, 5 Luer connectors respectively. (B) scalar shear stress distribution curves for VAD loops with a 90° T-connector and an ideal 90° angulation (1 Pa = 10 dyne/cm^2) [Color figure can be viewed at wileyonlinelibrary.com]

TABLE 1 Blood shear stress within the circulatory loops with the different number of Luer connectors

Number of connectors	Average blood shear (dyne/cm^2)	Increment (%)	Increment to baseline (%)	Peak blood shear (dyne/cm^2)	Increment (%)	Increment to baseline (%)
0	3.6930	–	–	28.9783	–	–
1	3.7260	0.90	0.90	29.2720	1.01	1.01
2	3.7753	1.35	2.23	30.9810	5.84	6.91
3	3.8067	0.83	3.08	31.1617	0.58	7.53
4	3.8480	1.09	4.20	31.3253	0.53	8.02
5	3.8930	1.17	5.42	33.1590	5.85	14.43

circulatory loop created a significant increase in shear stress of approximately 5.60%, compared to a 90° ideal angulation set-up (Table 2). Specifically, the shear stress distributions had different topographies at low shear stress (0-2 dyne/cm^2) range (Figure 4B). The peak shear stress increased by 236.00% with addition of a T-connector (significantly higher than peak shear stress of a straight Luer connector).

The scalar transport Eulerian method currently available in the literature has been found to accurately predict relative comparisons of platelet activation and hemolysis in MCS systems under various operating conditions. The platelet activation indexes (PAI) increased monotonically as the number of Luer connector increased (Figure 5). The PAI for the 5-connector loop was roughly 3.22% higher than that of 0-connector one. Though slightly increased, this value indicates the percentage of activated platelets from total platelets[39] for a single passage circulation in the loop. For the 90° scenario, the loop with a T-connector exhibited 28.84% higher PAI than a loop with ideal 90° angulation, revealing a significant higher platelet activation level.

To straightforwardly illustrate the impacts of additive loop components on platelet activation, contour plots of the PAI on wall of circulatory loops and on selective middle planes are shown in Figure 6 to show where platelets are expected to activate. The PAIs were normalized to the outlet value of each candidate circulation to show the special variation in each loop. From both scenarios, it is shown that the proximal side of angulations led to more platelet activations, due to changes of flow patterns.

In the various number of Luer connector case, it is noted from wall contour plots that luer ports and edges between connectors and tubes altered the topography of PAI. These impacts can be better revealed from middle plane contours that regions such as the luer ports and non-smooth turnings of tube have warmer color, which represent more platelet activations. For the 90° case, similar to the previous case, the luer ports and the bending of tube on the right side show high PAI. Besides, the T-connector lighted up larger areas (last subfigure in Figure 6) at the 90° angulation and downstream after that, than the ideal 90° loop.

3.2 | In vitro assessment of shear stresses

Specifically, two extreme situations, that is, 0-connector ($n = 6$) and 5-connector ($n = 4$), were investigated in vitro and results are shown in Figure 7A. The PAS in the 0-connector loop reached a "steady" state after 30 min, achieving an increase of only 4.3-fold (±1.3) after 60-minute of circulation. In contrast, the 5-connector loop exhibited a steeper platelet activation, with a 7.0-fold (±2.1) increase at 60-minutes. The difference in the elevation of the PAS levels of the two

TABLE 2 Blood shear stress within the circulatory loops testing 90° angulation

Loop	Average blood shear (dyne/cm^2)	Increment (%)	Peak blood shear (dyne/cm^2)	Increment (%)
90° ideal	3.5787	–	29.7177	–
90° T-connector	3.8863	5.60	99.8513	236.00

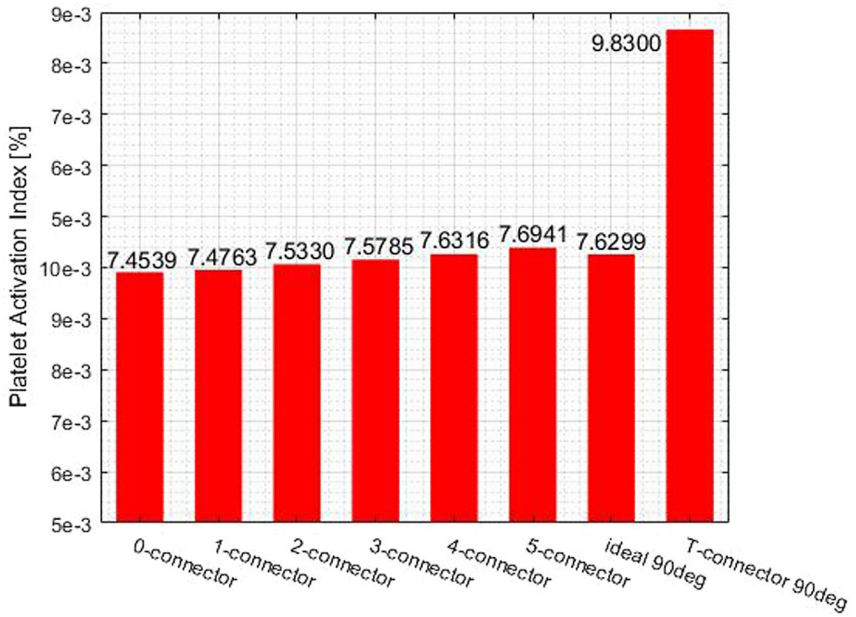

FIGURE 5 Comparison of the PAI between candidate circulation loops [Color figure can be viewed at wileyonlinelibrary.com]

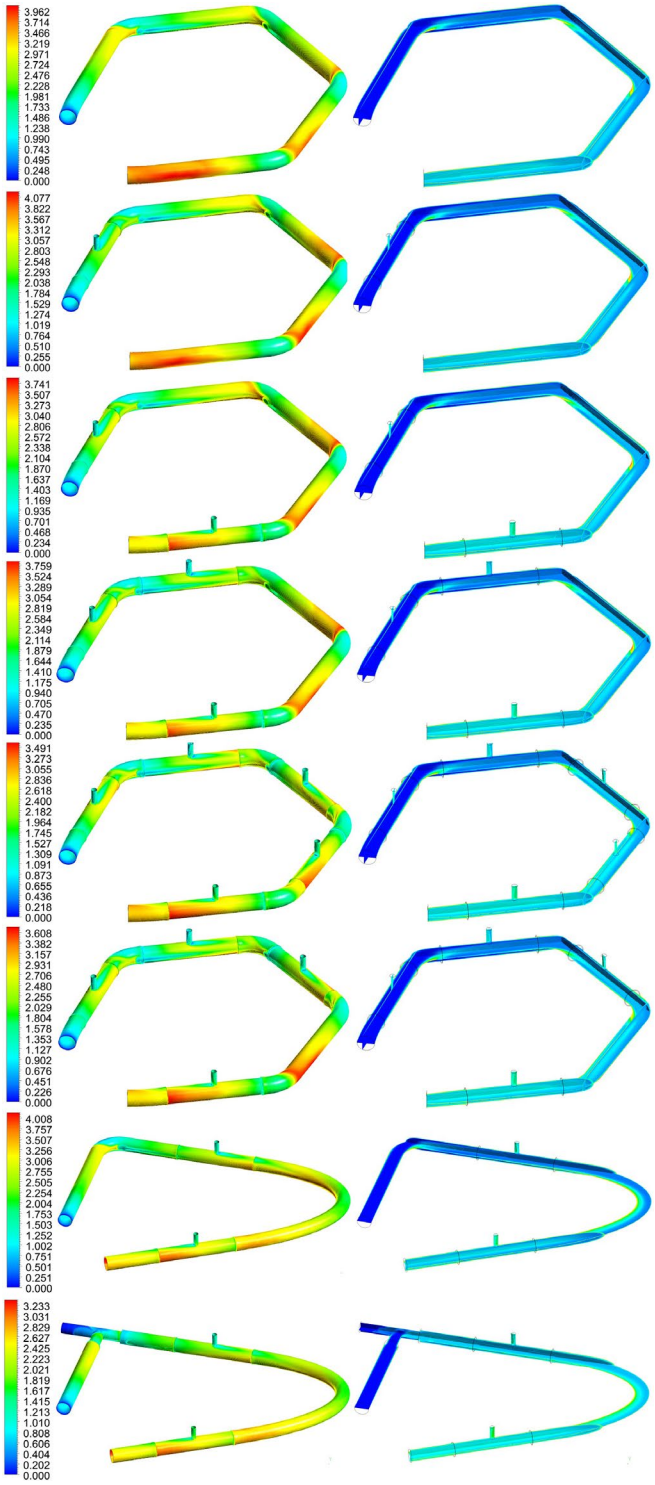

FIGURE 6 Contour plots of PAI normalized to the outlet value to show the special variation in each scenarios. Row 1 to row 8: VAD testing loops with 0, 1, 2, 3, 4, 5 Luer connectors, a loop with ideal 90° angulation, and a loop with a 90° T-connector, respectively. Column one to column two: contour on wall and contours on selective middle planes [Color figure can be viewed at wileyonlinelibrary.com]

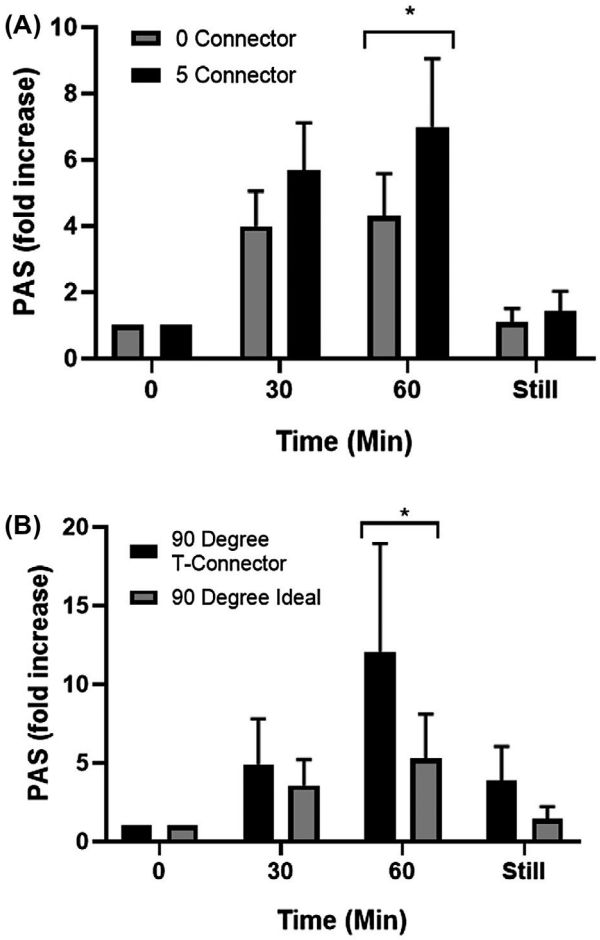

FIGURE 7 (A) Platelet activation measurements for 0 and 5 Luer connection VAD testing loops. (B) Platelet activation measurements for a 90° T-connector and an ideal 90° angulation VAD testing loops

conditions at 60 minutes was found to be significant (two-way ANOVA, $P = .023$). Both loops demonstrated increasing platelet activation as time progressed. The zero connector loop exhibited significant differences over the zero min time point by 30 minutes (two-way ANOVA, $P = .0013$ and $P > .0001$ respectively), while the five connector loop exhibited a significant difference over the zero minute time point by 30 minutes (two-way ANOVA, $P = .0317$). Further, with multiple connectors we noted that it was harder to remove air from the loop, potentially adding to an increase in platelet activation level. Nevertheless, in all experiments extreme care was taken and no evidence of contained air, bubbles or foam was detected for all studies reported. Regardless, the 5-connector loop still demonstrated higher platelet activation levels, compared with a zero connector loop, throughout the whole experiment duration, further suggesting the additional connectors indeed contribute to additive platelet activation.

Similarly, the PAS values correspond to expected platelet activation differences between the 90° T-connector loop ($n = 5$) and the ideal 90° angulation loop ($n = 5$) (Figure 7B). Both loops demonstrated increasing platelet activation as time progressed. Following 60 minutes circulation, the T-connector loop demonstrated significantly higher platelet activation over

zero minute samples. (two-way ANOVA, $P < .0001$). Addition of the T-connector introduced higher platelet activation across the experiment duration, especially between the 30 and 60 minutes interval. In contrast, the platelet activation level in the ideal 90° loop increased smoothly and slowly. After 60-minutes circulation, the PAS levels of the 90° T-connector loop increased 12.1-fold (±6.9), while the ideal 90° loop led to only 5.3-fold (±2.9) elevation (two-way ANOVA, $P = .0041$).

4 | DISCUSSION

In vitro assessment of MCS devices in blood, or blood constituent—that is, platelet, containing loops is an essential and widely utilized step to evaluate device thrombogenicity and overall hemocompatibility, in the overall natural history of advancing devices through design iterations and on to regulatory approval. Unfortunately, to date, device loops employed by academic and commercial groups are largely individually designed by a given lab or manufacturer without standardization, with a wide variety of constructs routinely employed. Here, we demonstrate via in silico and in vitro methods that individual loop elements, notably the number of Luer connectors, the presence of stopcocks and angulation, all impart additive shear stress to recirculating fluid and blood elements, thus activating more platelets. The in silico model predicts additive shear SA, leading to SMPA, as confirmed by our studies under "wet" in vitro conditions, and may confound the results of the test VAD or MCS device contained within that loop. Our studies confirm our hypothesis suspicion and raise a word of caution for the field. We again emphasize that while most careful workers will maintain consistency of loop design our experience in the field, working with individual groups, manufacturers, and the FDA has motivated this study as the addition of a connector here and a port there is often felt to be inconsequential—this work demonstrates the need for added caution, diligence, and exactness.

4.1 | In vitro loop studies

There is no standard method or FDA Guidance Document for appropriately designing and building a mock circulatory loop to minimize the blood damage and platelet activation induced by the loop itself, and to solely assess MCS hemocompatibility. Even though ASTM F 1841 provides some standard practices for loop preparations to investigate hemolysis of MCS devices, it only provides suggestions about general loop geometry and components to use. Details, such as how to connect components to avoid sharp edges, abrupt tubing size transitions, with narrowing and dilatations, or how to create any angulation, are lacking. Similarly, suggested positions as to where to install pressure sensors are not provided, as inexact positioning of these may lead to untoward results due to Bernoulli effects from these components as well.

Researchers have been working on developing mock circulatory loops to investigate MCS device performance for decades (continuous pumps,[18–22] pulsatile pumps[23–27]). However, these previous mock loops and studies were used only for hemodynamic and pressure-volume response determination and did not formally consider hemocompatibility or platelet activation. Ducko et al[43] developed a mock loop for hemolysis studies of artificial hearts using biocompatible materials, claiming that the loop was "not likely" to cause loop-induced blood damage without further explanation. Though Garrison et al[44] pointed out that an ideal testing loop should incorporate favorable geometry, that is, containing no sharp turns or sudden narrowings or dilatations, other possible loop components that may contaminate the results were not considered. Graf et al[45] constructed a loop to test a pulsatile TAH with the need of minimizing loop-induced hemolysis though similarly did not detail or explicitly consider contributions of loop geometry and loop elements to hemocompatibility. Many groups normally do not explicitly mention the consideration of avoiding loop-induced blood damage and they might accidently introduce those components. For instance, a standard loop similar to ASTM F 1841 set up by Berk et al[46] to evaluate LVAD hemolysis utilized two reducer connectors (similar to a nozzle) for the installation of a clamp on flow probe, which was studied and illustrated to induce hemolysis by FDA.[47]

Loop components and geometry certainly impact thrombogenicity. Some studies have suggested that loop geometry affects the thrombogenicity of the whole system. Chiu et al[28] studied this in silico and found that different anastomotic angles of inflow and outflow cannulas of a VAD do impact the overall system thrombogenic potential. Wu et al[48] numerically investigated and presented the effects of various fluid channel geometries on platelet activation and blood damage. Fuchs et al[49] analyzed the flow induced platelet activation from ECMO components such as cannulae and tubing connector using CFD.

4.2 | Advances of our studies

Our studies advance the following:

1. In silico models revealed that additive loop elements, such as Luer connectors or 90° T-connectors, alter total system shear stress and therefore impart stresses and SA, potentially leading to higher degree of platelet activation.
2. In vitro tests demonstrated that actual circulatory testing loops, replicating geometry, and components as those modeled in silico, in fact resulted in higher platelet activation levels with the addition of increasing number of loop components.

3. In silico CFD simulations can correlatively predict the extent of platelet activation in vitro. In vitro results on the contrary strongly support and confirm the in silico simulation results.

Instead of generic recommendations (eg, ISO 14708-5, ASTM F 1841), this article provides studies, analyses, and examples regarding defined circulatory loop geometries and additive loop components, to inform and assist design and fabrication of MCS device circulatory loops, which may provide a pathway toward establishment of a standard for consistency. It further emphasizes the need for maintenance of consistency of loop design throughout serial testing of a device, or during comparison to other predicates, without what may seem as innocuous additional loop elements mid-course which may unknowingly inject error from the loop itself.

5 | LIMITATION

The power law model assumes constant shear stress, while blood experiences dynamic shear stress in real applications. Also, the coefficients used by Ding et al[39] were established for high shear (25-350 Pa) and short exposure time (0.039-0.15 seconds) situations. Another set of coefficients developed by Sheriff et al[50] is suitable for low shear stress (1-7 Pa) but not short exposure time (1-4 minutes). Nonetheless, our study clearly demonstrates the quantitative tendency and that additive loop elements impact platelet activation. Further investigation, including advanced CFD/FSI simulation, will enhance these initial findings. Specifically, a more computationally intense and rigorous Lagrangian method, that is, DTE,[11] developed by our group, will be utilized in future studies to model blood as a two-phase fluid and integrate the sss with residence time along all possible platelet trajectories, considering platelet SA histories, to further extend the findings and impact of this study.

6 | CONCLUSION

The effects of additional loop components on additive shear stress in MCS device circulatory testing loops were explicitly studied via in silico and in vitro models. We observed that each additive component of conventional connectors commonly utilized in laboratory loop configurations does indeed impact generated shear stress. If several connectors are utilized the loop itself will impart shear stress, leading to inadvertent and erroneous characterization of a contained test MCS device. While most workers are careful in loop design, the addition of loop elements midstream in testing, or during comparative device analysis, has often been felt to be inconsequential. Our studies indicate the need for diligence here, and the significance of these elements as well. Careful design of testing loops, with in silico consideration of additive prothrombotic contributions of loop components and fixtures, will further improve the utility of current in vitro testing systems and approaches. Results from this study illustrate the need to develop standards—as to loop design and constituent components. They also emphasize the need to characterize and report on the loop at baseline, and to maintain consistency of design throughout a given testing run, or comparative device evaluation trial. This will allow elimination of the "noise" of the system and prevent additive contribution of shear from elements felt to be inconsequential, which quietly have impact.

ACKNOWLEDGMENT

We acknowledge support from the NIH U01 1U01HL131052-01A1 as well as from the Arizona Center for Accelerated Biomedical Innovation (ACABI) of the University of Arizona.

CONFLICT OF INTEREST

The authors declare that they have no conflicts of interest with the contents of this article.

ORCID

Mengtang Li https://orcid.org/0000-0002-3594-4808
Jawaad Sheriff https://orcid.org/0000-0002-1297-0739
Marvin J. Slepian https://orcid.org/0000-0002-7864-6691

REFERENCES

1. Benjamin EJ, Muntner P, Alonso A, Bittencourt MS, Callaway CW, Carson AP, et al. Heart disease and stroke statistics-2019 update: a report from the American Heart Association. Circulation. 2019;139:e56–528.
2. Kirklin JK, Naftel DC, Pagani FD, Kormos RL, Myers S, Acker MA, et al. Pump thrombosis in the Thoratec HeartMate II device: an update analysis of the INTERMACS Registry. J Heart Lung Transplant. 2015;34:1515–26.
3. Kreuziger LB, Massicotte MP. Mechanical circulatory support: balancing bleeding and clotting in high-risk patients. ASH Education Program Book. 2015;2015:61–8.
4. Gurbel PA, Shah P, Desai S, Tantry US. Antithrombotic strategies and device thrombosis. Cardiol Clin. 2018;36:541–50.
5. Alemu Y, Bluestein D. Flow-induced platelet activation and damage accumulation in a mechanical heart valve: numerical studies. Artif Organs. 2007;31:677–88. https://doi.org/10.1111/j.1525-1594.2007.00446.x.
6. Sheriff J, Tran PL, Hutchinson M, DeCook T, Slepian MJ, Bluestein D, et al. Repetitive hypershear activates and sensitizes platelets in a dose-dependent manner. Artif Organs. 2016;40:586–95. https://doi.org/10.1111/aor.12602.
7. Slepian MJ, Sheriff J, Hutchinson M, Tran P, Bajaj N, Garcia JGN, et al. Shear-mediated platelet activation in the free flow: perspectives on the emerging spectrum of cell mechanobiological mechanisms mediating cardiovascular implant thrombosis. J Biomech. 2017;50:20–5. https://doi.org/10.1016/j.jbiomech.2016.11.016.

8. Kang J, Zhang D, Motomura T, Acker M, Atluri P, Bartoli CR. LVAD device design features and operational settings minimize von Willebrand factor degradation. J Heart Lung Transplant. 2016; 35:S81.
9. Roka-Moiia Y, Palomares DE, Sheriff J, Bluestein D, Slepian MJ. MCS shear-medicated platelet activation does not cause integrin GPIIbIIIa activation, rather shedding and microparticle generation. J Heart Lung Transplant. 2018;37:S162.
10. American Society for Testing and Materials. ASTM F1841-97. Standard practice for assessment of hemolysis in continuous flow blood pumps. West Conshohocken, PA: ASTM; 2004.
11. Dimasi A, Rasponi M, Sheriff J, Chiu W-C, Bluestein D, Tran PL, et al. Microfluidic emulation of mechanical circulatory support device shear-mediated platelet activation. Biomed Microdevices. 2015;17:117.
12. Girdhar G, Xenos M, Alemu Y, Chiu W-C, Lynch BE, Jesty J, et al. Device thrombogenicity emulation: a novel method for optimizing mechanical circulatory support device thromboresistance. PLoS ONE 2012;7:e32463.
13. Bluestein D, Girdhar G, Einav S, Slepian MJ. Device thrombogenicity emulation: a novel methodology for optimizing the thromboresistance of cardiovascular devices. J Biomech. 2013;46:338–44.
14. Chiu W-C, Girdhar G, Xenos M, Alemu Y, Soares JS, Einav S, et al. Thromboresistance comparison of the HeartMate II ventricular assist device with the device thrombogenicity emulation-optimized HeartAssist 5 VAD. J Biomech Eng. 2014;136:021014.
15. Xenos M, Girdhar G, Alemu Y, Jesty J, Slepian M, Einav S, et al. Device Thrombogenicity Emulator (DTE)—design optimization methodology for cardiovascular devices: a study in two bileaflet MHV designs. J Biomech. 2010;43:2400–9.
16. FDA. General considerations for animal studies for cardiovascular devices—guidance for industry and FDA staff [Internet]. Available from: www.fda.gov/regulatory-information/search-fda-guidance-documents/general-considerations-animal-studies-cardiovascular-devices-guidance-industry-and-fda-staff. Accessed July 9, 2019.
17. FDA. General considerations for animal studies for medical devices [Internet]. Available from: www.fda.gov/regulatory-information/search-fda-guidance-documents/general-considerations-animal-studies-medical-devices. Accessed July 9, 2019.
18. Bearnson GB, Olsen DB, Khanwilkar PS, Long JW, Allaire PE, Maslen EH. Pulsatile operation of a centrifugal ventricular assist device with magnetic bearings. ASAIO J. 1996;42:M620–4.
19. Iijima T, Inamoto T, Nogawa M, Takatani S. Control of centrifugal blood pump based on the motor current. Artif Organs. 1997;21:655–60.
20. Pantalos GM, Altieri F, Berson A, Borovetz H, Butler K, Byrd G, et al. Long-term mechanical circulatory support system reliability recommendation: American Society for Artificial Internal Organs and The Society of Thoracic Surgeons: long-term mechanical circulatory support system reliability recommendation. Ann Thorac Surg. 1998;66:1852–9.
21. Kikugawa D. Evaluation of cardiac function during left ventricular assist by a centrifugal blood pump. Artif Organs. 2000;24:632–5.
22. Timms D, Hayne M, McNeil K, Galbraith A. A complete mock circulation loop for the evaluation of left, right, and biventricular assist devices. Artif Organs. 2005;29:564–72. https://doi.org/10.1111/j.1525-1594.2005.29094.x.
23. Rosenberg G, Phillips WM, Landis DL, Pierce WS. Design and evaluation of the Pennsylvania State University mock circulatory system. ASAIO J. 1981;4:41–9.
24. Lukic B, Weiss W. The effect of pump rate and filling on hemolysis in a pulsatile left ventricular assist device (LVAD). Proceedings of the IEEE 28th Annual Northeast Bioengineering Conference (IEEE Cat. No.02CH37342), 2002:181–2.
25. Ohashi Y, de Andrade A, Nosé Y. Hemolysis in an electromechanical driven pulsatile total artificial heart. Artif Organs. 2003;27:1089–93.
26. Pantalos GM, Koenig SC, Gillars KJ, Giridharan GA, Ewert DL. Characterization of an adult mock circulation for testing cardiac support devices. ASAIO J. 2004;50:37–46.
27. Ito K, Sudo T, Shima T, Kouno Y, Ohnishi Y, Tanaka T, et al. Characteristics of spiral vortex pump driven by two different drivers. Biocybern Biomed Eng. 2007;27:121–32.
28. Chiu W-C, Alemu Y, McLarty AJ, Einav S, Slepian MJ, Bluestein D. Ventricular assist device implantation configurations impact overall mechanical circulatory support system thrombogenic potential. ASAIO J. 2017;63:285–92.
29. Kazui T, Zhang A, Greenberg J, Itoh A, Tran PL, Keith AD, et al. Left ventricular assist device inflow angle and pump positional change over time adverse impact on left ventricular assist device function. Ann Thorac Surg. 2016;102:1933–40.
30. Marom G, Bluestein D. Lagrangian methods for blood damage estimation in cardiovascular devices—how numerical implementation affects the results. Expert Rev Med Devices. 2016;13:113–22.
31. Consolo F, Sferrazza G, Motolone G, Contri R, Valerio L, Lembo R, et al. Platelet activation is a preoperative risk factor for the development of thromboembolic complications in patients with continuous-flow left ventricular assist device. Eur J Heart Fail. 2018;20:792–800. https://doi.org/10.1002/ejhf.1113.
32. Fuchs G, Berg N, Broman LM, Prahl WL. Modeling sensitivity and uncertainties in platelet activation models applied on centrifugal pumps for extracorporeal life support. Sci Rep. 2019;9:8809.
33. Menter F. Zonal two equation k-w turbulence models for aerodynamic flows. 23rd Fluid Dynamics, Plasmadynamics, and Lasers Conference, Orlando, FL, U.S.A: American Institute of Aeronautics and Astronautics; 1993. https://doi.org/10.2514/6.1993-2906.
34. Menter FR. Two-equation eddy-viscosity turbulence models for engineering applications. AIAA J. 1994;32:1598–605.
35. Hariharan P, D'Souza G, Horner M, Malinauskas RA, Myers MR. Verification benchmarks to assess the implementation of computational fluid dynamics based hemolysis prediction models. J Biomech Eng. 2015;137:094501. https://doi.org/10.1115/1.4030823.
36. Apel J, Paul R, Klaus S, Siess T, Reul H. Assessment of hemolysis related quantities in a microaxial blood pump by computational fluid dynamics. Artif Organs. 2001;25:341–7.
37. Faghih MM, Keith SM. Extending the power-law hemolysis model to complex flows. J Biomech Eng. 2016;138:124504. https://doi.org/10.1115/1.4034786.
38. Giersiepen M, Wurzinger LJ, Opitz R, Reul H. Estimation of shear stress-related blood damage in heart valve prostheses—in vitro comparison of 25 aortic valves. Int J Artif Organs. 1990;13: 300–6.
39. Ding J, Chen Z, Niu S, Zhang J, Mondal NK, Griffith BP, et al. Quantification of shear-induced platelet activation: high shear stresses for short exposure time. Artif Organs. 2015;39:576–83. https://doi.org/10.1111/aor.12438.
40. Jesty J, Bluestein D. Acetylated prothrombin as a substrate in the measurement of the procoagulant activity of platelets: elimination of the feedback activation of platelets by thrombin. Anal Biochem. 1999;272:64–70.

41. Nobili M, Sheriff J, Morbiducci U, Redaelli A, Bluestein D. Platelet activation due to hemodynamic shear stresses: damage accumulation model and comparison to in vitro measurements. ASAIO J. 2008;54:64–72.
42. Schulz-Heik K, Ramachandran J, Bluestein D, Jesty J. The extent of platelet activation under shear depends on platelet count: differential expression of anionic phospholipid and factor Va. Pathophysiol Haemost Thromb. 2005;34:255–62.
43. Ducko CT, McGregor ML, Rosenberg G, Pierce WS. The effect of valve type and drive line dP/dt on hemolysis in the pneumatic ventricular assist device. Artif Organs. 1994;18:454–60.
44. Garrison LA, Frangos JA, Geselowitz DB, Lamson TC, Tarbell JM. A new mock circulatory loop and its application to the study of chemical additive and aortic pressure effects on hemolysis in the Penn State electric ventricular assist device. Artif Organs. 1994;18:397–407. https://doi.org/10.1111/j.1525-1594.1994.tb02222.x.
45. Gräf F, Finocchiaro T, Laumen M, Mager I, Steinseifer U. Mock circulation loop to investigate hemolysis in a pulsatile total artificial heart. Artif Organs. 2015;39:416–22.
46. Berk ZBK, Zhang J, Chen Z, Tran D, Griffith BP, Wu ZJ. Evaluation of in vitro hemolysis and platelet activation of a newly developed maglev LVAD and two clinically used LVADs with human blood. Artif Organs. 2019;43:870–9. https://doi.org/10.1111/aor.13471.
47. Malinauskas RA, Hariharan P, Day SW, Herbertson LH, Buesen M, Steinseifer U, et al. FDA benchmark medical device flow models for CFD validation. ASAIO J. 2017;63:150–60. https://doi.org/10.1097/MAT.0000000000000499.
48. Wu J, Yun BM, Fallon AM, Hanson SR, Aidun CK, Yoganathan AP. Numerical investigation of the effects of channel geometry on platelet activation and blood damage. Ann Biomed Eng. 2011;39:897–910.
49. Fuchs G, Berg N, Broman LM, Prahl WL. Flow-induced platelet activation in components of the extracorporeal membrane oxygenation circuit. Sci Rep. 2018;8:13985.
50. Sheriff J, Soares JS, Xenos M, Jesty J, Slepian MJ, Bluestein D. Evaluation of shear-induced platelet activation models under constant and dynamic shear stress loading conditions relevant to devices. Ann Biomed Eng. 2013;41:1279–96.

How to cite this article: Li M, Walk R, Roka-Moiia Y, et al. Circulatory loop design and components introduce artifacts impacting in vitro evaluation of ventricular assist device thrombogenicity: A call for caution. *Artif Organs*. 2020;00:1–12. https://doi.org/10.1111/aor.13626